

Thermalization of Hadrons via Hagedorn States

M. Beitel, K. Gallmeister, and C. Greiner

*Institut für Theoretische Physik, Goethe-Universität Frankfurt am Main,
Max-von-Laue-Str. 1, 60438 Frankfurt am Main, Germany*

Hagedorn states are characterized by being very massive hadron-like resonances and by not being limited to quantum numbers of known hadrons. To generate such a zoo of different Hagedorn states, a covariantly formulated bootstrap equation is solved by ensuring energy conservation and conservation of baryon number B , strangeness S and electric charge Q . The numerical solution of this equation provides Hagedorn spectra, which enable to obtain the decay width for Hagedorn states needed in cascading decay simulations. A single (heavy) Hagedorn state cascades by various two-body decay channels subsequently into final stable hadrons. All final hadronic observables like masses, spectral functions and decay branching ratios for hadronic feed down are taken from the hadronic transport model UrQMD. Strikingly, the final energy spectra of resulting hadrons are exponential showing a thermal-like distribution with the characteristic Hagedorn temperature.

In the 60's of the last century physicists were puzzled by the diversity of different hadron species growing with beam energy. Before the emergence of quantum chromodynamics (QCD) as the theory of strong interactions many ideas came up to explain these findings. R. Hagedorn [1] proposed to describe the variety of particles found by a common mass spectrum, now better known as Hagedorn spectrum, arising in the framework of a "statistical bootstrap model". In the infinite mass limit this spectrum is exponentially rising where the slope is determined by the Hagedorn 'temperature' T_H . Above this temperature the partition function of a strongly interacting hadronic system with such an exponential growth of states diverges and a new state of matter, the 'Quark Gluon Plasma' (QGP), is assumed to be realized. One of the most challenging problems is to understand how this phase transition exactly occurs and which new properties this new state of matter has. One possible tool to investigate microscopically a phase transition from hadronic to partonic phase is the application and generation of Hagedorn states being created in multiparticle collisions [2–6]. These resonances belong to the continuous part of the Hagedorn spectrum and are allowed to have any mass larger than that of the heaviest known hadron and also any quantum numbers as long as they are compatible with their mass. Such Hagedorn states can alter the occurrence of various phases from hadronic to deconfined partonic matter [7–12].

The abundant appearance of Hagedorn states in the vicinity of T_H helps to explain how chemical equilibrium of hadrons is achieved on timescales significantly smaller than the typical lifetime of a fireball ($t \approx 10 \text{ fm}/c$). In Refs. [4–6], the authors examined chemical equilibration times of (multi-) strange (anti-) baryons at Relativistic Heavy Ion Collider (RHIC) energies by solving a set of coupled rate equations. It was assumed, that most abundant mesons (pions, kaons) 'cluster' to Hagedorn states which in turn decay into hyperons driving them quickly into equilibrium. For example, the chemical equilibration times of protons, kaons and lambdas within this approach

are of the order of 1-2 fm/c. The inclusion of Hagedorn states in a hadron resonance gas model provides a lowering of the speed of sound, c_s , at the phase transition and being in good agreement with lattice calculations [13–16]. In addition, by comparing calculations with inclusion of Hagedorn states to calculations without them, a significant lowering of the shear viscosity to entropy ratio, η/s , is observed [13, 15, 17, 18]. The inclusion of Hagedorn states creates a minor dependence of the thermal fit parameters of particle ratios on the Hagedorn temperature, T_H , which is assumed to be equal to T_C [19].

In order to describe the hadronization of jets in e^+e^- annihilation events, different scenarios were developed during the 70's and 80's of the last century: While the first one assumes independent parton fragmentation [20], the fundamental objects of the second approach are color strings [21]. Finally, the basic assumption of the latter is that partons tend to cluster in color singlet states from the very beginning of the generated event. These cluster then decay to smaller ones, until some cut-off scale is reached and hadrons are formed [22, 23]. An explicit application of the "statistical bootstrap model" has been used to calculate several properties of particles stemming from decays of hadronic fireballs being created in relativistic heavy ion collisions [24]. In the framework of RQMD multi-particle collisions and their decays were introduced by the so called particle clusters a particle system can separate into provided the existence of separable interactions in the relativistic particle dynamics exists. This clustering is for example fulfilled for colored quarks and gluons [25]. Another statistical approach within the microcanonical ensemble addressed the hadronization of quark matter droplets [26]. A further statistical treatment of Hagedorn states was performed in Ref. [27] by forcing detailed balance between creation and decay of Hagedorn states with a simplistic description of the spectrum in the low mass region. The authors made then the extreme assumption of one single heavy Hagedorn state subsequently decaying into stable hadrons giving rise to measured particle multiplicities at RHIC and Super Pro-

ton Synchrotron (SPS) energies. The several terms like 'quark matter droplets', 'clusters' or 'fireballs' may all be identified with possible Hagedorn states.

The present work formulates the whole zoo of Hagedorn states and their decay properties, as created in binary collisions within the microscopic hadronic transport simulation program UrQMD [28]. Multiplicities (and their ratios) of stable hadrons stemming from cascading decay simulations of massive Hagedorn states are calculated. Additionally energy distribution of the decay products are examined and it is shown that all hadrons stemming from that cascade follow the Boltzmann distribution resulting in a thermalized hadron resonance gas. Contrary to the well-known non-covariant bootstrap equation [29], here a covariantly formulated [30] bootstrap equation

$$\tau_{\vec{C}}(m) = \frac{R^3}{3\pi m} \sum_{\vec{C}_1, \vec{C}_2} \iint dm_1 dm_2 \tau_{\vec{C}_1}(m_1) m_1 \quad (1)$$

$$\times \tau_{\vec{C}_2}(m_2) m_2 p_{cm}(m, m_1, m_2) \delta^{(3)}(\vec{C} - \vec{C}_1 - \vec{C}_2),$$

is used, which ensures strict energy and quantum number conservation, $\vec{C} = (B, S, Q)$. (R stands for the radius of the Hagedorn state's volume as discussed below.) The main idea behind any such bootstrap equation is the "statistical bootstrap model" which postulates that fireballs consist of fireballs which in turn consist of fireballs etc., resulting in a common spectrum with the remarkable feature that it grows approximately exponentially in the infinite mass limit. The present approach is restricted to two constituents only making up a Hagedorn state because the focus is put on $2 \leftrightarrow 1$ processes only. With this the principle of detailed balance can be applied, which can be implemented into a standard hadronic transport framework. This restriction is backed by the Hagedorn state decay probability into n particles, $P(n) = (\ln 2)^{n-1} / (n-1)!$, yielding a probability for the decay into two particles of 69%, into three particles of 24% etc. [29]. The bootstrap equation (1) in general is a highly non-linear integral equation of Volterra type which can be solved analytically for some special cases [31, 32]. Here the basic input are the spectral functions provided by the hadronic table of UrQMD consisting of 55 different baryons and 32 different mesons [28], calling for a numerical solution.

Thus one starts by inserting known hadron spectral functions on the r.h.s. of Eq. (1) resulting into first Hagedorn states on the l.h.s. of this equation. In the subsequent steps, these created Hagedorn states serve as constituents in addition to the known sources. In each step, quantum number conservation $\vec{C} = \vec{C}_1 + \vec{C}_2$ is assured. In this fashion one proceeds by increasing the mass by steps of $\Delta m = 0.01$ GeV. Unfortunately, the computation time increases with mass according m^8 , since more and more constituents have to be taken into account.

Thus the applicability of this approach is limited to the region $m \leq 8$ GeV.

Given the Hagedorn spectra, $\tau_{\vec{C}}(m)$, one is able to derive a formula for the total decay width of the Hagedorn states. For this purpose one modifies the general two body decay formula [33] to take the mass degeneration into account. In the general formulae for cross section and decay width, the creation, $|\mathcal{M}_c|^2$, and the decay matrix elements, $|\mathcal{M}_d|^2$, appear which for Hagedorn states are at first unknown. By demanding the principle of detailed balance $|\mathcal{M}_c|^2 = |\mathcal{M}_d|^2$, one eventually leads to

$$\Gamma_{\vec{C}}(m) = \frac{\sigma}{2\pi^2 \tau_{\vec{C}}(m)} \sum_{\vec{C}_1, \vec{C}_2} \iint dm_1 dm_2 \tau_{\vec{C}_1}(m_1) \tau_{\vec{C}_2}(m_2)$$

$$\times p_{cm}(m, m_1, m_2)^2 \delta^{(3)}(\vec{C} - \vec{C}_1 - \vec{C}_2). \quad (2)$$

Here, by connecting the radius parameter R of (1) with the cross section σ of (2) via $\sigma = \pi R^2$ the size of the Hagedorn state is connected with its production and decay properties. This decay width formula of the Hagedorn state provides one with the various two-body branching ratios needed for calculation of hadronic multiplicities in cascade simulations.

The numerical solution of the given bootstrap equation for a mesonic, non-strange and electrically neutral ($B=S=Q=0$) Hagedorn spectrum for two different typical radii ($R_1 = 0.8$ fm, $R_2 = 1.0$ fm) is presented in Fig. 1. In the same figure also spectra for baryonic non-strange and electrically charged states ($B=1, S=0, Q=1$) are shown. All Hagedorn spectra rise exponentially for masses ≥ 1.5 GeV with different slopes for different radii, but for $m < 1.5$ GeV they all include and thus fit the 'hadronic' part of the spectrum. Here lies the major advantage of the present approach since ad hoc assumptions of the kind $\tau(m) = f(m) \exp(m/T_H)$ with most used pre-functions $f(m) = Am^{-b}$ or $f(m) = A(m^2 + m_r^2)^{-b}$ fail to describe the low mass region of the spectrum. The slopes of the exponential part depend strongly on the size of the Hagedorn state since in a larger one more states can be counted than in a smaller one. The slope parameter is the well known Hagedorn temperature T_H being extracted with the fit function $\tau_{\text{fit}}(m) = Am^{-b} \exp(m/T_H)$, yielding $T_H = 0.145$ GeV for $R = 1.0$ fm and $T_H = 0.162$ GeV for $R = 0.8$ fm. Thus smaller Hagedorn states exhibit a larger Hagedorn temperatures depending on the energy density. The Hagedorn temperature range is basically the same for mesonic and baryonic spectra in our model in contrast to [34] where 'mesonic' and 'baryonic' Hagedorn temperatures differ significantly because they were extracted not from the continuous part of the Hagedorn spectrum but from its low-mass region.

In Fig. 2 the total decay width of a mesonic, non-strange and electrically uncharged ($B=S=Q=0$) Hagedorn state for same two different radii as before is shown.

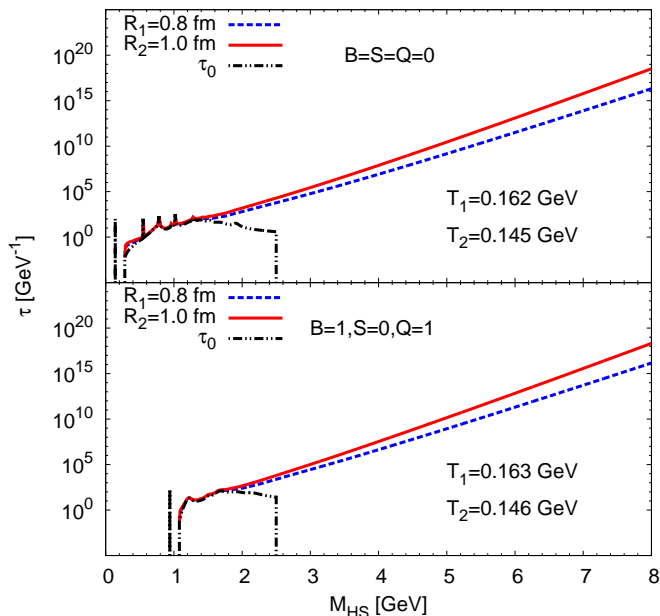


FIG. 1: Mesonic ($B = S = Q = 0$) (up) and baryonic ($B = 1, S = 0, Q = 1$) (down) Hagedorn spectra for two different radii with corresponding (fitted) Hagedorn temperatures. The black line represents the sum of spectral functions of hadrons with the given quantum numbers.

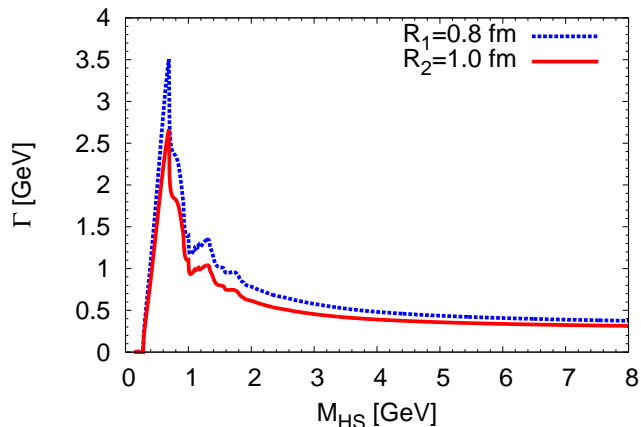


FIG. 2: Total decay width of charge neutral Hagedorn state for two different radii.

The total decay width of a Hagedorn state consists of three different contributions, where the first one considers only hadrons, the second hadrons and Hagedorn states, and the third one only Hagedorn states in the outgoing channel. The peak in the mass range of $M_{HS} = 0-2$ GeV comes mainly from the first contribution, because in this mass range the phase space for pure hadronic decay is largest [35]. The height of the peak depends on the number of hadronic pairs which quantum numbers all sum up to the quantum number of the Hagedorn state they are building up, being large for $B = S = Q = 0$. An-

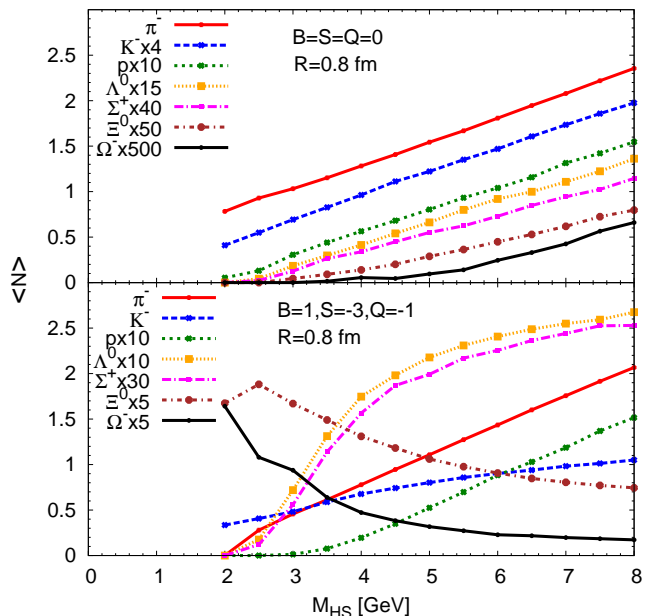


FIG. 3: Hadronic multiplicities after a cascade decay of Hagedorn state with radius $R = 0.8$ fm and $B = S = Q = 0$ (up) and $B = 1, S = -3, Q = -1$ (down) and the following hadronic feed down.

other remarkable feature is that for both radii the total decay width tends to a constant value depending only on R . This finding is expected by causality where the lifetime of resonance of dimension R against decay should be roughly the light-travel time across R .

Having the numerous branching ratios at hand, one is able to calculate hadronic multiplicities stemming from Hagedorn state decays. Here one starts with some initial heavy Hagedorn state which decays subsequently down until hadrons are left only. Among those also non stable resonances might appear which further undergo a hadronic feed down leaving us with light and stable hadrons with respect to the strong force like pions, kaons, etc.. All hadronic properties used here were taken from the transport model UrQMD [28].

Calculated multiplicities for some uncharged ($B = S = Q = 0$) initial Hagedorn state are shown in Fig. 3. One observes a linear dependence of all multiplicities on the initial Hagedorn state mass where the magnitude depends on the available phase space for each hadron. Thus in a decay of a charge neutral Hagedorn state π^- dominate which have to be produced in pairs mostly with π^+ since exact charge conservation is enforced. Kaons, especially K^- , are even stronger suppressed not only of their larger mass but also due to the fact that they have to conserve both electric charge and strangeness. For the baryons presented the same argumentation holds since both have to conserve baryon number B and additionally electric charge Q for proton and strangeness S for Λ . For the multistrange hyperons Ξ^0 and Ω^- the production suppression is even

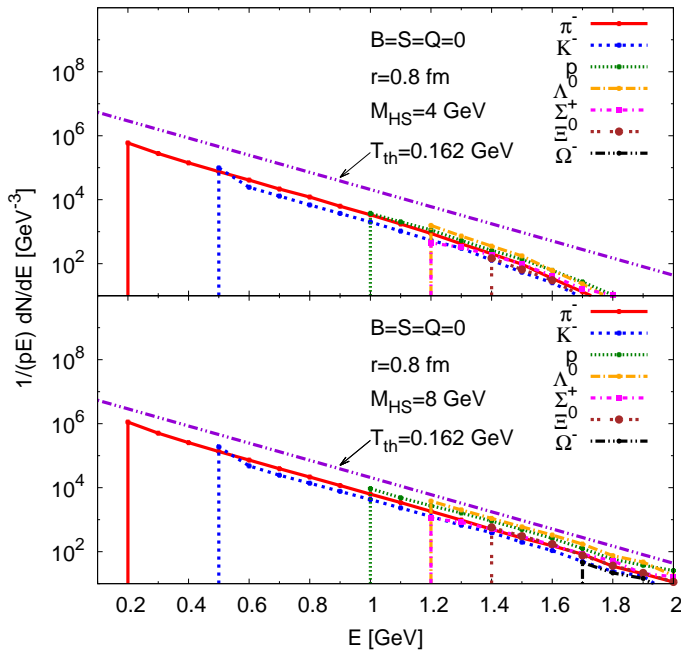


FIG. 4: Energy spectra of hadrons stemming from cascade decay of charge neutral Hagedorn state with radius $R = 0.8$ fm and initial mass $M_{HS} = 4$ GeV and $M_{HS} = 8$ GeV.

stronger. This has to be contrasted with the results for a baryonic, multi-strange and electrically charged ($B = 1, S = -3, Q = -1$) Ω^- -like Hagedorn state also shown in Fig. 3. Now the choice of Hagedorn state's initial quantum numbers is reflected in the preference of baryon production although they are much heavier than the presented mesons. Especially the abundance of hyperons (Ω^-, Ξ^0) compared to the case discussed before is striking since the easiest way to conserve the initial quantum numbers is the production of one $\Omega^-\pi^0$ - or one $\Xi^0 K^-$ pair where on the other hand the phase space for all other hadrons with different quantum numbers is suppressed now. Hence exact conservation of quantum numbers always causes a competition between hadron's phase space and its quantum numbers.

The energy distribution of hadrons stemming from Hagedorn state decays in these cascading decay simulations are some further striking result. They are shown in Fig. 4 for an uncharged ($B = S = Q = 0$) Hagedorn state with initial mass $M_{HS} = 4$ GeV and also $M_{HS} = 8$ GeV.

The energy distributions for all species presented follow some exponential law with the same slope being independent on Hagedorn state's initial mass. Thus the energies of these final hadrons are distributed akin to Boltzmann which in turn means that their distribution obey a 'thermal' microcanonical state at a temperature being $T_{th} = 0.162$ GeV. This is remarkable, since this is exactly the Hagedorn temperature (cf. Fig. 1). The Hagedorn temperature T_H was nothing but a slope parameter to fit the exponential part of the Hagedorn spec-

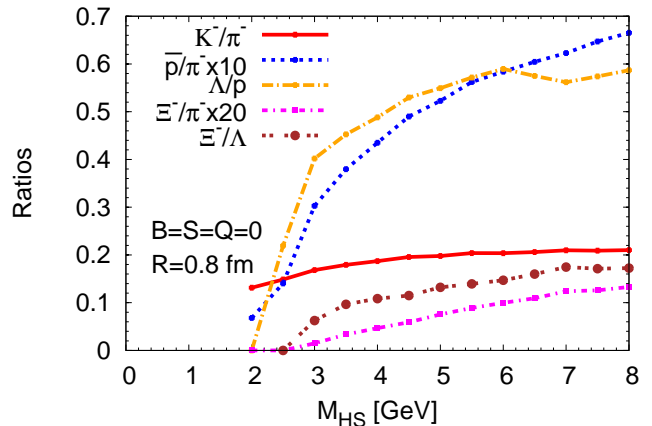


FIG. 5: Hadronic ratios stemming from cascade decay of charge neutral Hagedorn state with radius $R = 0.8$ fm.

trum, where on the other hand T_{th} is a physical of the created hadron resonance gas. We started with a bootstrap formulae with no introduction of temperatures at all and obtain a 'thermalized' decay with a temperature being the Hagedorn temperature.

In Fig. 5 various ratios of most interesting state hadrons stemming from a decay of an uncharged ($B = S = Q = 0$) Hagedorn state with $R = 0.8$ fm are presented. Numerical values for the multiplicity ratios for Hagedorn state masses of 4 GeV and 8 GeV are listed in table I and compared to experimental results from ALICE at LHC [36–38].

	experiment	4 GeV	8 GeV
K^-/π^-	0.149 ± 0.016	0.187	0.210
\bar{p}/π^-	0.045 ± 0.005	0.043	0.066
Λ/π^-	0.036 ± 0.005	0.021	0.038
Λ/\bar{p}	0.778 ± 0.116	0.494	0.579
Ξ^-/π^-	0.0050 ± 0.0006	0.0023	0.0066
Ω^-/π^-	$(8.7 \pm 1.7) \cdot 10^{-4}$	$0.86 \cdot 10^{-4}$	$5.60 \cdot 10^{-4}$

TABLE I: Comparison of particle multiplicity ratios from theory vs. experiment [36–38]. Calculated values are listed for Hagedorn state masses of 4 GeV and 8 GeV.

In smaller systems like e^+e^- or p - p lighter color neutral blobs or clusters may be created which solely decay [22, 23]. For such small systems one had employed thermal descriptions incorporating a strangeness suppression factor γ_s [39]. On the other hand, in relativistic heavy ion collisions larger objects may be generated which then also interact and are decaying and regenerated. This may lead to a faster equilibration close to the phase transition [4, 6].

Summarizing, such a finding gives new insight into the microscopic and thermal-like hadronization in ultrarelativistic e^+e^- (see eg. [39]), hadron-hadron-, and also es-

pecially in heavy ion collisions: An implementation of the presented Hagedorn state decays in addition to their production mechanisms into the transport approach UrQMD offers a new venue for allowing hadronic multiparticle collisions in a consistent scheme being important in the vicinity of the deconfinement transition. Understanding faster thermalization and chemical equilibration, but also microscopic transport properties can be thoroughly investigated in future [35].

This work was supported by the Bundesministerium für Bildung und Forschung (BMBF), the HGS-HIRe and the Helmholtz International Center for FAIR within the framework of the LOEWE program launched by the State of Hesse. Numerical computations have been performed at the Center for Scientific Computing (CSC).

-
- [1] R. Hagedorn, *Nuovo Cim. Suppl.* **3**, 147 (1965).
 [2] C. Greiner and S. Leupold, *J. Phys. G* **27**, L95 (2001).
 [3] C. Greiner, P. Koch-Steinheimer, F. M. Liu, I. A. Shovkovy, and H. Stoecker, *J. Phys. G* **31**, S725 (2005).
 [4] J. Noronha-Hostler, C. Greiner, and I. A. Shovkovy, *Phys. Rev. Lett.* **100**, 252301 (2008).
 [5] J. Noronha-Hostler, C. Greiner, and I. Shovkovy, *J.Phys.G* **37**, 094017 (2010).
 [6] J. Noronha-Hostler, M. Beitel, C. Greiner, and I. Shovkovy, *Phys. Rev. C* **81**, 054909 (2010).
 [7] L. Moretto, K. Bugaev, J. Elliott, and L. Phair, *Europhys.Lett.* **76**, 402 (2006).
 [8] I. Zakout, C. Greiner, and J. Schaffner-Bielich, *Nucl. Phys. A* **781**, 150 (2007).
 [9] I. Zakout and C. Greiner, *Phys. Rev. C* **78**, 034916 (2008).
 [10] L. Ferroni and V. Koch, *Phys. Rev. C* **79**, 034905 (2009).
 [11] K. Bugaev, V. Petrov, and G. Zinovjev, *Phys. Rev. C* **79**, 054913 (2009).
 [12] A. Ivanytskyi, K. Bugaev, A. Sorin, and G. Zinovjev, *Phys.Rev.E* **86**, 061107 (2012).
 [13] J. Noronha-Hostler, J. Noronha, and C. Greiner, *Phys. Rev. Lett.* **103**, 172302 (2009).
 [14] A. Majumder and B. Muller, *Phys. Rev. Lett.* **105**, 252002 (2010).
 [15] J. Noronha-Hostler, J. Noronha, and C. Greiner, *Phys. Rev. C* **86**, 024913 (2012).
 [16] A. Jakovac, *Phys. Rev. D* **88**, 065012 (2013).
 [17] M. Gorenstein, M. Hauer, and O. Moroz, *Phys. Rev. C* **77**, 024911 (2008).
 [18] K. Itakura, O. Morimatsu, and H. Otomo, *J.Phys.G* **35**, 104149 (2008).
 [19] J. Noronha-Hostler, H. Ahmad, J. Noronha, and C. Greiner, *Phys. Rev. C* **82**, 024913 (2010).
 [20] R. Field and R. Feynman, *Nucl. Phys. B* **136**, 1 (1978).
 [21] B. Andersson, G. Gustafson, G. Ingelman, and T. Sjostrand, *Phys. Rept.* **97**, 31 (1983).
 [22] B. Webber, *Nucl. Phys. B* **238**, 492 (1984).
 [23] G. Marchesini, B. Webber, G. Abbiendi, I. Knowles, M. Seymour, et al., *Comput. Phys. Commun.* **67**, 465 (1992).
 [24] R. Hagedorn and J. Rafelski, *Phys.Lett.B* **97**, 136 (1980).
 [25] H. Sorge, H. Stoecker, and W. Greiner, *Annals Phys.* **192**, 266 (1989).
 [26] K. Werner and J. Aichelin, *Phys. Rev. C* **52**, 1584 (1995).
 [27] S. Pal and P. Danielewicz, *Phys. Lett. B* **627**, 55 (2005).
 [28] S. Bass, M. Belkacem, M. Bleicher, M. Brandstetter, L. Bravina, et al., *Prog.Part.Nucl.Phys.* **41**, 255 (1998).
 [29] S. C. Frautschi, *Phys. Rev. D* **3**, 2821 (1971).
 [30] E. Byckling and K. Kajantie, *Particle Kinematics* (John Wiley & Sons, London, 1973), ISBN 0471128856.
 [31] J. Yellin, *Nucl. Phys. B* **52**, 583 (1973).
 [32] R. Hagedorn and I. Montvay, *Nucl. Phys. B* **59**, 45 (1973).
 [33] J. Beringer et al. (Particle Data Group), *Phys. Rev. D* **86**, 010001 (2012).
 [34] W. Broniowski, W. Florkowski, and L. Y. Glozman, *Phys. Rev. D* **70**, 117503 (2004).
 [35] M. Beitel, K. Gallmeister, and C. Greiner, in preparation (2014).
 [36] B. Abelev et al. (ALICE Collaboration), *Phys. Rev. C* **88**, 044910 (2013).
 [37] B. B. Abelev et al. (ALICE Collaboration), *Phys. Rev. Lett.* **111**, 222301 (2013).
 [38] B. B. Abelev et al. (ALICE Collaboration), *Phys. Lett. B* **728**, 216 (2014).
 [39] F. Becattini, *Z.Phys.C* **69**, 485 (1996).